Electronic transport characterization of $Sc@C_{82}$ single-wall carbon nanotube peapods

A. L. Cantone,[1] M. R. Buitelaar,[1,a)] C. G. Smith,[1] D. Anderson,[1] G. A. C. Jones,[1] S. J. Chorley,[1] C. Casiraghi,[2] A. Lombardo,[2] A. C. Ferrari,[2] H. Shinohara,[3] A. Ardavan,[4] J. Warner,[5] A. A. R. Watt,[5] K. Porfyrakis,[5] and G. A. D. Briggs[5]
[1]*Cavendish Laboratory, University of Cambridge, Cambridge, CB3 0HE, United Kingdom*
[2]*Engineering Department, University of Cambridge, Cambridge CB3 0FA, United Kingdom*
[3]*Department of Chemistry, Nagoya University, Nagoya 464-8602, Japan*
[4]*Clarendon Laboratory, Oxford University, Oxford OX1 3PU, United Kingdom*
[5]*Department of Materials, Oxford University, Oxford OX1 3PH, United Kingdom*

(Received 30 April 2008; accepted 26 August 2008; published online 31 October 2008)

We present electrical transport and Raman measurements on individual single-wall carbon nanotubes filled with the paramagnetic metallofullerene $Sc@C_{82}$. We find nearly all devices to be metallic *p*-type conductors, which we tentatively attribute to bandstructure modification of the nanotubes by the encapsulated $Sc@C_{82}$ molecules. At low temperatures the peapod devices behave as quantum dots and transport is shown to be quantum coherent over distances of at least ~100 nm. Kondo features are observed at the lowest measurement temperatures of 50 mK. Our results are of fundamental interest because of the long spin coherence times of the unpaired electrons on the $Sc@C_{82}$ molecules and the possibility this offers for studying one-dimensional spin chains in carbon nanotubes. © *2008 American Institute of Physics*. [DOI: 10.1063/1.3000443]

I. INTRODUCTION

Single-wall carbon nanotubes (SWNTs) possess unique electronic and mechanical properties, which are of wide interest from both an applied and fundamental physics viewpoint. As is well established, as-grown carbon nanotubes are either semiconducting or metallic depending on their exact atomic arrangement. Of importance for applications in (opto)electronics is the bandgap of semiconducting nanotubes, which is usually fixed by, and inversely proportionally to, the nanotube diameter.[1] An interesting approach toward modification of the electronic structure of carbon nanotubes is the insertion of (endohedral) fullerenes in the nanotubes, resulting in nanotube peapods.[2,3] Several recent studies on nanotube peapod field effect transistors (FETs) demonstrated that incorporating fullerenes such as C_{60}, C_{78}, and C_{90}, as well as metallofullerenes such as $Dy@C_{82}$, $Gd@C_{82}$, $Ti_2@C_{80}$, and $Ce_2@C_{80}$ modify the bandgap of semiconducting nanotubes in a stable and reproducible way.[4,5] To date, however, there has been limited work on the spin properties of paramagnetic endohedral fullerenes in carbon nanotubes. Metallofullerenes such as $Sc@C_{82}$, $Y@C_{82}$, and $La@C_{82}$ have hybridized orbitals between the metal dopant and the fullerene cage and this leads to an unpaired electron, primarily delocalized across the C_{82} cage with a long spin coherence time as observed in, e.g., pulsed electron spin resonance (ESR) experiments on $Sc@C_{82}$ material in deoxygenated deuterated toluene.[6] SWNTs encapsulating paramagnetic endohedral fullerenes are also of fundamental interest for the possibility to investigate one-dimensional spin chains, which might have quantum information process (QIP) applications.[7] Here we present detailed transport and Raman experiments on individual $Sc@C_{82}$@SWNT peapods. We show that there is a marked difference between the room-temperature gate characteristics of filled and unfilled nanotubes, which is tentatively interpreted as the result of bandstructure modification of the nanotube by the $Sc@C_{82}$ molecules. Of importance for QIP applications is our observation that despite the strong effect on the room-temperature characteristics, the metallofullerenes do not introduce strong backscattering in the nanotubes and at low temperatures, transport is found to be phase coherent over extended distances. These measurements also present a first step toward electrically detected magnetic resonance experiments[8] on $Sc@C_{82}$@SWNT devices, which will allow us to probe the spin properties of individual $Sc@C_{82}$ molecules, rather than an ensemble of (at least) 10^{12} molecular spins, as necessary for conventional ESR techniques.

II. MATERIAL

SWNTs produced by arc discharge were purchased from Aldrich and purified via the following steps:[9] (1) microwave for 5 min, (2) heat in the air at 325 °C for 1 h, (3) reflux in 37% hydrochloric acid for 2 h, (4) filter and wash with de-ionized water, (5) reflux in hydrogen peroxide for 2 h, (6) filter and wash with de-ionized water, and (7) dry at 200 °C and store in a nitrogen dry-box. $Sc@C_{82}$ was made using arc discharge and purified by high performance liquid chromatography (HPLC) according to methods described in the literature.[10] Nanotube peapods were made by taking a dry mixture of $Sc@C_{82}$ and SWNT in a quartz ampule, evacuating and sealing at 10^{-4} Torr. The ampule was heated at 400 °C and after 4 days the mixture was washed and filtered with carbon disulphide and toluene to remove any excess fullerene molecules from the outside of the nanotubes.[11] Samples for electron microscopy were prepared by ultrasoni-

a)Electronic mail: mrb51@cam.ac.uk.

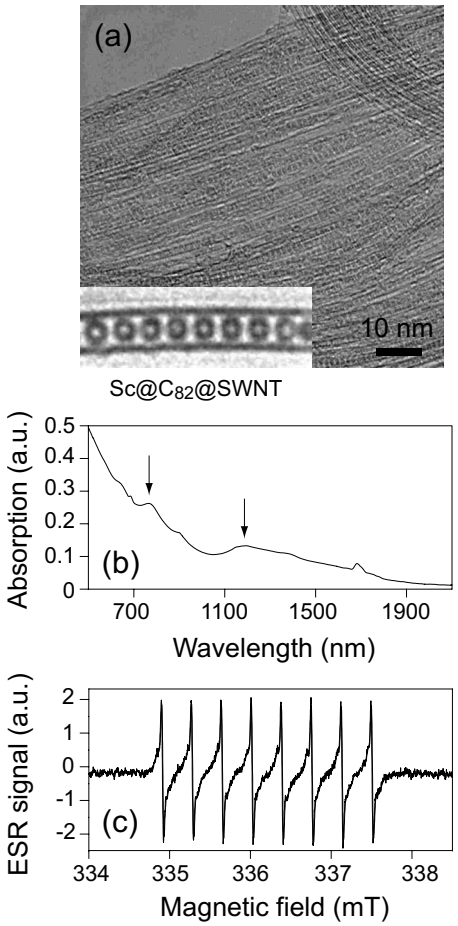

FIG. 1. (a) TEM image of $Sc@C_{82}@SWNT$ peapods. The high resolution image (inset) shows an individual peapod. (b) UV-vis-NIR absorption spectrum of $Sc@C_{82}$ in CS_2. The small peak appearing at 1700 nm is probably due to trace amounts of toluene in the sample. (c) ESR measurement of $Sc@C_{82}$ in CS_2.

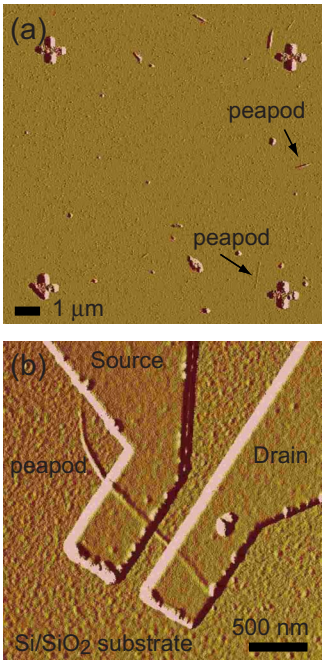

FIG. 2. (Color online) (a) AFM image of a dispersion of $Sc@C_{82}@SWNT$ peapods. The alignment marks are used to locate the peapods on the substrate. (b) AFM image of a single contacted peapod. The Pd source and drain electrodes are separated by about 300 nm. The Si/SiO_2 substrate is used as a gate electrode.

cation of dilute dispersions in methanol, which were dropped onto lacey carbon coated copper grids and then analyzed using a JEOL JEM-4000EX high resolution tunnel electron microscope (TEM) operating at an accelerating voltage of 100 kV. Figure 1(a) shows a TEM image of a bundle of repeatedly purified SWNTs filled with $Sc@C_{82}$ metallofullerenes to form peapods. A high degree of filling of the interior of the SWNTs with the $Sc@C_{82}$ can be seen from this image. TEM analysis of several areas of the sample allowed an estimation of ~70%–90% filling of the nanotubes. In the inset of Fig. 1(a) a high resolution transmission electron microscopy image is presented and shows a single SWNT filled with fullerenes. The ultraviolet-visible-near infrared (UV-vis-NIR) optical absorption spectrum of the $Sc@C_{82}$ fullerenes in CS_2 solution is shown in Fig. 1(b) and two peaks are observed at 1190 and 760 nm. These are indicative of the Sc^{2+} oxidation state of the metallofullerene and confirm the formation of purified $Sc@C_{82}$.[10] Figure 1(c) shows the ESR spectrum of the $Sc@C_{82}$ in CS_2 solution with eight hyperfine splitting (hfs) lines (hfs constant of 0.38 mT) that match the $Sc@C_{82}$. The mass spectrum of the $Sc@C_{82}$ purified by HPLC and used in the peapod production gives a single peak at 1029.85 m/z. This confirms the high purity isolation of $Sc@C_{82}$ using multistage recycling HPLC. Overall, the characterization performed in Fig. 1 proves that a single isomer of the spin-active metallofullerene $Sc@C_{82}$ has been isolated with a high degree of purity and then used to form peapod structures with an excellent filling ratio.

III. DEVICE FABRICATION

A crucial step in the fabrication of nanotube devices is the deposition of tubes onto a substrate. Typically, the raw material consists of nanotubes in the form of long, tangled ropes. The goal is to deposit individual tubes a few microns long with the desired density, but technical difficulties lie in separating and cutting the tubes forming the ropes and depositing them uniformly onto the substrate. We achieved this [see Fig. 2(a)] by placing ~1 μg of tube material in a few ml of dichloroethane and suspending it using an ultrasonic bath. We found that the result depends critically on the agitation time and efficiency.

Suspensions of single tubes and thin ropes are obtained after ~60 min of agitation, giving the solvent a light gray color. Afterwards we dip our substrate (doped Si with 500 nm of SiO_2 on top) in the suspension for a few seconds and then rinse it with isopropanol (IPA). The tubes stick by van der Waals forces to the substrate, which is then blown dry with air. Nanotube depositions have mostly been investigated by atomic force microscopy (AFM) but occasionally using a scanning electron microscope (SEM) and Raman spectroscopy. The electron source of the SEM is a field emission gun operated at 1 kV acceleration voltage.[12] We find that most individual nanotube peapods have a length of <1 μm (which is much shorter than the raw nanotubes), presumably the result of the acid treatment necessary to remove (mag-

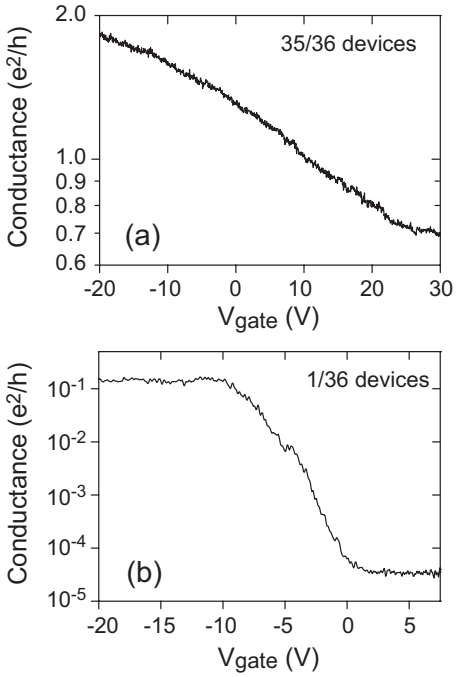

FIG. 3. (a) Conductance as a function of gate voltage for an individual $Sc@C_{82}@SWNT$ peapod measured at room temperature. The peapod shows only slight *p*-type behavior and no insulating state could be reached (up to 30 V of gate). These data are representative for 35 out of the 36 devices measured at room temperature. (b) Only one device out of the 36 showed clear semiconducting behavior. This curve has been offset by 5×10^{-5} e^2/h for clarity.

netic) impurities from the nanotube material and the subsequent sonication. Only nanotube peapods with apparent diameters $\lesssim 1.5$ nm, as determined by AFM, were selected for electrical characterization.

After having located the nanotube peapods with respect to alignment marks [Fig. 2(a)] a polymethyl methacrylate resist layer is spun onto the chip and baked for 30 min at 150 °C. The desired electrode pattern is then transferred onto the chip using a LEICA VB6 UHR electron-beam lithography system operated at a 100 kV acceleration voltage. The pattern is developed using a mixture of methyl ethyl ketone (MEK), methyl isobutyl ketone (MIBK), and IPA in the ratio MEK:MIBK:IPA 1:5:15 for about 25 s, followed by thermal evaporation of 40 nm of palladium (Pd) and lift-off in acetone. An example of a finished device is shown in Fig. 2(b).

IV. RESULTS

A. Room temperature behavior

We performed room-temperature two-terminal dc transport measurements on 36 $Sc@C_{82}@SWNT$ devices. In all measurements we varied the electrochemical potential of the nanotubes by applying a gate voltage V_g to the back of the Si substrates. Figure 3 shows representative measurements of the conductance versus gate voltage. Almost all devices (35 out of 36) followed the behavior shown in Fig. 3(a), i.e., decreasing *p*-type conductance with increasing positive V_g. With the exception of the one measurement shown in Fig. 3(b), we were not able to deplete any $Sc@C_{82}@SWNT$ device completely of charge, going up to voltages of $V_g = 40$ V. This is in marked contrast to empty carbon nanotubes for which 2/3 are expected to be semiconducting.[13] Indeed, we have measured many (>25) empty carbon nanotube devices, grown by chemical vapor deposition,[14] of which roughly 80% could be completely depleted of charge, usually within 10 V gate bias. The precise ratio of semiconducting to metallic tubes for the unfilled arc-discharge material used here (i.e., before encapsulation of the $Sc@C_{82}$ molecules) could not be determined precisely. Nevertheless, optical absorption spectra (not shown) for the unfilled nanotubes show that both semiconducting and metallic tubes with diameters between 1.3–1.5 nm are present. The presence of both semiconducting and metallic tubes also follows from transport and Raman experiments on the unfilled nanotube material (see Sec. V below).

The measurements on the device shown in Fig. 3(b), which has undergone the same treatment as all other peapod devices, also show that our gate electrode is clearly effective (a result which also follows from measurements shown in Figs. 4 and 5, see below). Based on our AFM measurements and low-temperature transport experiments (see below) we expect the majority of devices to consist of individual nanotube peapods rather than bundles or ropes of this material. Note that, even for small bundles ($\lesssim 5$ nanotubes) of empty nanotubes one would expect a significantly larger number of devices to be insulating at large positive gate voltages than observed in our experiments. Overall, this is therefore a strong indication that the unconventional room-temperature transport characteristics of the peapods are the result of the encapsulation of $Sc@C_{82}$ in the nanotubes.

It is instructive to compare these results with experiments on other (metallo)fullerene peapods. Recent studies of nanotube peapod FETs have shown a strong dependence of electronic transport on the size of the encapsulated fullerenes. Little bandgap modification for semiconducting peapods was found for encapsulation of C_{60}, a reduced bandgap for C_{78} and complete metallic behavior for C_{92}.[4] The electronic properties could be further tuned using metallofullerenes: the more charge transfer occurring inside the metallofullerene, the smaller the bandgap of the nanotube peapods.[5] This bandgap modification has also been observed in scanning tunneling microscopy experiments[15] and has been attributed to orbital hybridization between the SWNT and fullerene states.[16,17] It seems reasonable to assume that this will also be the case in our experiments.

Given the Sc^{2+} oxidation state of the $Sc@C_{82}$ metallofullerenes used in our experiments we would, following the findings by Shimada *et al.*,[5] expect a reduced but nevertheless finite bandgap for the $Sc@C_{82}@SWNT$ peapods. Moreover, recent density functional theory (DFT) calculations[18] for $Sc@C_{82}@SWNT$, using the semiconducting (7,14) SWNT, also predict an observable band gap. This discrepancy between our experiments and theory is not clear at present. However, we note that the results might depend sensitively on the nanotube diameter (and the corresponding separation between the fullerenes and nanotube wall). An-

other consideration is that electron transfer between the Pd electrodes and nanotube peapod is not accounted for in the DFT calculation in Ref. 18.

B. Low-temperature behavior

Following the room-temperature experiments, we have measured the differential conductance (dI/dV) as a function of V_g and V_{sd} for twelve different devices at temperatures of 50 mK, 1.4, and 4.2 K. As is the case for unfilled carbon nanotubes, the coupling between the electrodes and the nanotube peapods varies between devices, giving rise to different physical phenomena. Figure 4 shows the results for two devices of the geometry given in Fig. 2(b) that have a relatively low conductance at low temperatures (of order $10^{-3}e^2/h$). Coulomb diamonds and excited states are clearly resolved in the measurement of Fig. 4(a). From the size of the Coulomb diamonds we extract a charging energy $U_C \sim 15$ meV and a zero-dimensional level spacing $\Delta E \sim 4$ meV. From the Coulomb diamonds it is also possible to determine the total device capacitance $C_\Sigma = e^2/U_C$, which yields $C_\Sigma \sim 11$ aF, and a gate efficiency $C_g/C_\Sigma \sim 0.1$, where C_g is the gate capacitance.

These values are not uncommon for carbon nanotube quantum dots of length 300 nm (the source-drain separation).[19] Indeed, if we assume the conventional dispersion relation for an (unfilled) metallic carbon nanotube, this implies a quantum dot of length $L = hv_F/4\Delta E \sim 200$ nm, where we have used $v_F = 8 \times 10^5$ m/sec for the Fermi velocity. Note that for nanotube peapods, the dispersion relation is not *a priori* clear since the encapsulated $Sc@C_{82}$ is (given our room-temperature results) expected to modify the nanotube band structure. Nevertheless, the good agreement with the conventional dispersion relation indicates that the Fermi velocity is similar to that of undoped metallic nanotubes for this device. The fact that we observe quantum coherent transport over extended distances is encouraging for future experiments. Note that coherent transport has also been reported for low-temperature experiments on individual $C_{60}@$SWNT peapods.[20,21] However, given that $Sc@C_{82}$ appears to have a much greater effect on the bandstructure than C_{60}, the similar behavior observed here is still surprising.

As is the case for empty carbon nanotubes, we have also frequently observed transport characteristics as shown in Fig. 4(b), which are much less regular in appearance. The suppression of the linear-response conductance and frequent occurrence of negative differential conductance (arrows) are indicative of multiple (two or three) quantum dots in series. From the level spacing measured for six different devices, we deduce (assuming the dispersion relation above) an average mean free path of ~ 100 nm, i.e., still much longer than the separation between individual $Sc@C_{82}$ molecules. Note that very similar results, i.e., both single dot[20,21] and multidot behavior[22] have been reported for $C_{60}@$SWNT. The cause of disorder in our devices is not known but it is reasonable to assume that the strong etching of the devices, not only shortens the carbon nanotubes but also introduces some disorder. Nanotube growth free from magnetic impurities is now available, which eliminates the need for strong etching.[23] This will allow longer and less disordered nanotubes to be studied in future experiments.

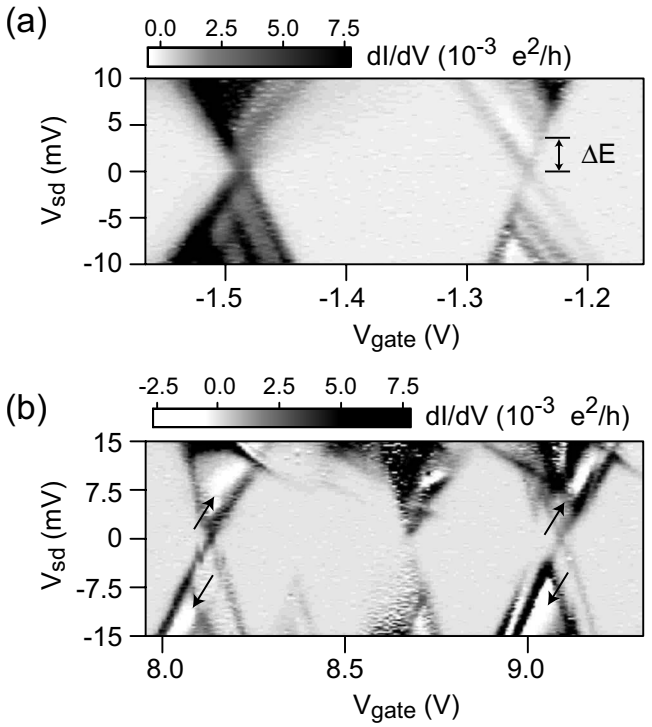

FIG. 4. (a) Grey scale representation of the differential conductance (dI/dV) as a function of source drain (V_{sd}) and gate voltage (V_g) at $T=1.4$ K for an individual $Sc@C_{82}@$SWNT peapod. The excitation lines are consistent with transport through a single quantum dot between the source and drain electrodes. (b) Grey scale representation of the differential conductance as a function of source drain and gate voltage at $T=4.2$ K for a different $Sc@C_{82}@$SWNT peapod. The suppression of the linear-response conductance and occurrence of negative $d//dV$ indicate that this device consists of multiple quantum dots in series.

Additional evidence that transport in $Sc@C_{82}@$SWNT peapods is quantum coherent over extended distances comes from transport experiment on devices in which the peapod is strongly coupled to the Pd electrodes, as shown in Fig. 5. The conductance in this devices is large, of order e^2/h. In contrast to weakly coupled devices, conductance features appear at $V_{sd}=0$ mV at certain Coulomb diamonds, see Fig. 5(a). These high-conductance ridges are a manifestation of the Kondo effect occurring when the number of electrons on the quantum dot is odd, as previously observed in unfilled carbon nanotubes[24,25] and $C_{60}@$SWNT peapods.[20,26] The total spin on the quantum dot is difficult to determine in this measurement, which is complicated by additional sharp features (at e.g., $V_g=-15.5$ V) that resemble Fano resonances as also seen in empty nanotubes.[27] Nevertheless, the high-conductance Kondo ridges observed in Fig. 5(a) are direct evidence that transport is quantum coherent over the entire length between the electrodes (300 nm), consistent with our findings for the weakly coupled devices (Fig. 4).

The magnetic field (B) dependence of the Kondo features follows the expected behavior[24] in which the high-conductance ridges split into components at $V_{sd} = \pm g\mu_B B/e$, where g is the Landé factor and μ_B is the Bohr magneton, see Fig. 5(b). From the magnetic field dependence of the Kondo features we obtain $g = 2.0 \pm 0.1$.

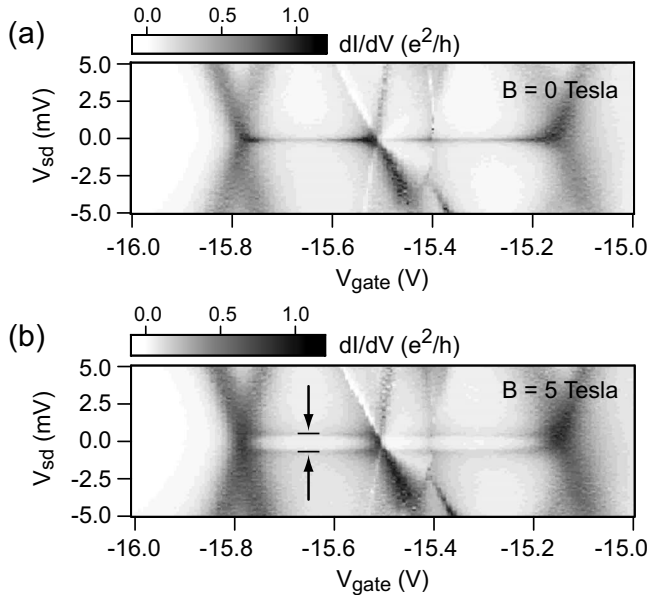

FIG. 5. (a) Grey scale representation of the differential conductance (dI/dV) as a function of source drain (V_{sd}) and gate voltage (V_g) of an $Sc@C_{82}@SWNT$ peapod measured at $T=50$ mK and $B=0$ T. The high-conductance ridges at $V_{sd}=0$ mV are a manifestation of the Kondo effect. (b) Grey scale representation of the differential conductance as a function of source drain and gate voltage at $B=5$ T for the same gate range as panel (a). The Kondo ridges split into components at $V_{sd}=\pm g\mu_B B/e$ when a magnetic field is applied.

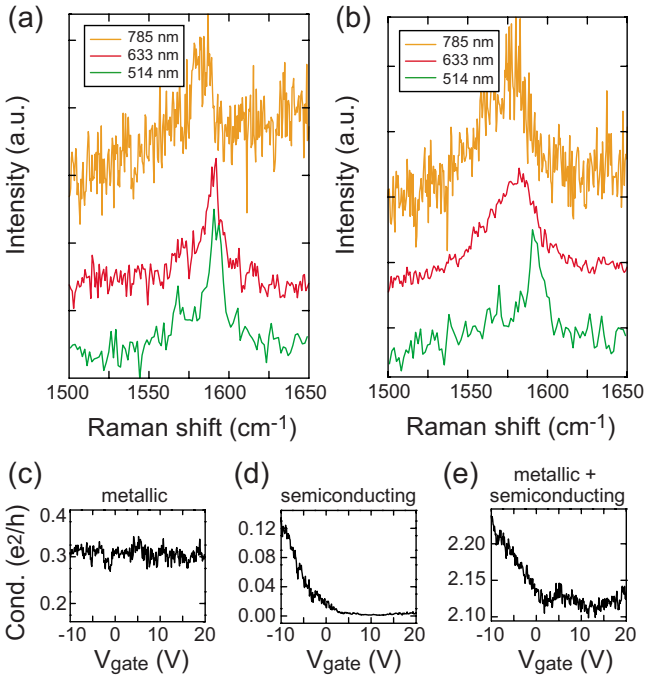

FIG. 6. (Color online) First order Raman spectra of two unfilled carbon nanotube devices measured at 785, 633, and 514 nm. (a) Spectrum of an individual semiconducting nanotube. (b) Spectrum indicative of a small bundle of mixed composition. (c)–(e) Transport measurements of three different unfilled nanotube devices. We observed the characteristic behavior of individual metallic nanotubes, individual semiconducting nanotubes, as well as nanotube bundles of mixed composition. The Raman spectra corresponding to the devices of panels (d) and (e) are shown in panels (a) and (b), respectively.

V. RAMAN SPECTROSCOPY

Raman spectroscopy is a fast and nondestructive method for the characterization of carbon materials and nanotubes in particular.[28] In the 1550–1590 cm^{-1} region, the Raman spectra of SWNTs are characterized by the presence of two distinct features: the so-called G^+ and G^- peaks. These originate from the splitting of the E_{2g} phonon of graphene in modes tangential (TO) and longitudinal (LO), with respect to the tube axis. The G^- is the LO mode in metallic tubes, while it is the TO mode in semiconducting ones, and vice-versa for the G^+ peak.[29–31] In semiconducting tubes, both peaks appear as sharp Lorentzians. The G^+ peak is usually more intense than the G^-, and its position is nearly independent on the tube's diameter, whereas the position of the G^- peak decreases for decreasing diameter.[29,31] On the other hand, in metallic tubes, the G^- peak is usually rather intense, very broad, and downshifted with respect to its counterpart in semiconducting tubes.[29] Doping changes the peaks' positions and widths.[32–34] In the 1300–1400 cm^{-1} range the D peak can be present. This is common to all carbon materials and is an indication of disorder.[30,35–37] While this requires a defect for its activation, the second order, $2D$ peak, is always present in all carbons.[38,39] The other prominent features in the Raman spectrum of SWNTs are the radial breathing modes,[40–43] which allow the determination of the SWNT diameter.

Raman spectra are measured at 514, 633, and 785 nm excitations in backscattering geometry, using a Renishaw micro-Raman 1000 spectrometer and a 100X objective. The finite number of wavelengths does not guarantee we can always be resonant with the individual tubes we measure. The spectral resolution is ~3 cm^{-1}. In order to avoid damage, the power on the sample is kept below 0.5 mW. The positioning of the tubes under the laser spot is achieved and maintained using a piezoelectric stage. The incident light is linearly polarized. The angle between the tube axis (determined by AFM measurements) and the light polarization is always kept as close as possible to zero. This is done by rotating the sample or by using a Fresnel Rhomb polarizer. No analysis of the polarization of the scattered light is performed. For simplicity, the spectra are fitted by using Lorentzians for all peaks.

To investigate the effect of the $Sc@C_{82}$ molecules inside the nanotubes on the Raman spectroscopy, we first discuss Raman measurements on unfilled carbon nanotubes for comparison. Apart from the filling procedure, the unfilled nanotubes have been exposed to the same processing steps, as described in Secs. II and III. We measured eight unfilled, but contacted, SWNTs. The AFM measurements of the diameters ($\lesssim 1.5$ nm) would in principle indicate the presence of only a single nanotube for the majority of devices. Of these, five gave a significant Raman intensity for at least one of the used wavelengths, but only one of them had a clear metallic G peak Raman signature. Figures 6(a) and 6(b) show two representative cases. Figure 6(a) is a measurement on a single individual semiconducting tube, as validated by direct transport measurements, see Fig. 6(d). It shows the typical sharp G peak expected in this case.[29,31] On the other hand, the Raman spectra in Fig. 6(b) change with excitation wavelength. While the 514 nm spectrum is indicative of a semi-

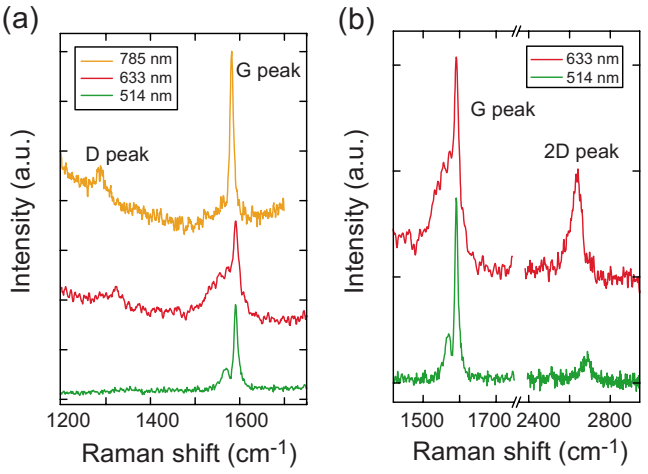

FIG. 7. (Color online) Raman spectra of a $Sc@C_{82}$@SWNT device. (a) First order Raman spectrum measured at 785, 633, and 514 nm. (b) First and second order Raman spectrum measured at 633 and 514 nm.

conducting tube, that at 633 nm has a typical metallic shape.[29,31] A variation from an apparently metallic to an apparently semiconducting shape for changing excitation wavelength was previously observed,[44] and assigned to an effect of the double resonance of the *G* peak.[44] Alternatively, such spectral change is expected when a single metallic tube is measured away from single resonance.[29,31] However, in this sample the conductance drops rapidly when the gate voltage is increased from negative values to about 0 V and then stays roughly constant [see Fig. 6(e)] as would be expected from a combination of semiconducting and metallic tubes. Thus, even though AFM measurements would point to the presence of a single nanotube, transport data indicate the sample in Fig. 6(b) to be more consistent with a small bundle, including at least one metallic and one semiconducting tube. We believe that the variation in the Raman spectrum observed in Fig. 6(b) reflects this mixed composition, rather than a single nanotube with changing spectral shape as a function of excitation wavelength.[44] Thus, the results of Ref. 44 should be reconsidered.

A total of 13 $Sc@C_{82}$@SWNT samples was also investigated. Unfortunately, in this case we could not independently measure both Raman and transport on the same devices. Of these, 11 tubes were detected for at least one of the available excitation wavelengths. In particular, most nanotubes were detected at 514 and 633 nm and only one tube or small bundle was seen for all three wavelengths. We could not measure clear radial breathing modes at these excitation energies. Figure 7 plots the Raman spectra measured on the sample detected at all three wavelengths. A weak *D* peak is seen at 785 and 633 nm, indicative of the presence of defects. The shape of the *G* peak changes with the excitation wavelength. The G^- is broad at 785 and 633 nm. This broad G^- indicates the presence of a metallic tube.[31,34,44] The same was observed on most of the tubes: six tubes over eight show a broad G^- peak at 633 nm, while at 514 nm, eight tubes over nine show a sharp G^-. At 785 nm only five tubes are detected, two of them with a broad G^-. In total, eight of the 11 samples show a metallic character for at least one excitation wavelength, in agreement with transport measurements on similar peapods. Again, the change in shape at different excitation wavelengths can be explained either as a single tube going slightly off-resonance[31,44] or by the presence of more than one tube in the sample (but, given the AFM measurements, the sample would at most consist of two or three tubes).

From the measured Raman spectra it is unclear if the metallic behavior is intrinsic (the empty tube was already metallic) or due to a band-gap closure as a consequence of the metallofullerene. However, compared to the empty tubes, we find significantly more metallic lineshapes, for at least one excitation wavelength, in the case of the filled tubes, which supports the latter scenario.

VI. CONCLUSIONS

In conclusion, we have measured the electrical transport properties of SWNTs filled with the paramagnetic metallofullerene $Sc@C_{82}$. Nearly all devices behave as metallic *p*-type conductors, consistent with Raman spectroscopy measurements. Low-temperature measurements show that transport in the nanotube peapods is quantum coherent over distances of at least ~100 nm. More experimental and theoretical work is necessary for a detailed understanding of the effect of the $Sc@C_{82}$ molecules on the bandstructure of the nanotubes.

ACKNOWLEDGMENTS

We thank Ling Ge, John Jefferson, and John Morton for discussion. G.A.D.B. thanks EPSRC for a Professional Research Fellowship (Grant No. GR/S15808/01). This research is part of QIP IRC (Grant No. GR/S82176/01). C.C. acknowledges the Oppenheimer and the Alexander von Humboldt Foundation. A.C.F. acknowledges the Royal Society and European Research Council grant Nanopots.

[1] H. Kataura, Y. Kumazawa, Y. Maniwa, I. Umezu, S. Suzuki, Y. Ohtsuka, and Y. Achiba, Synth. Met. **103**, 2555 (1999).
[2] A. Monthioux, Carbon **40**, 1809 (2002).
[3] R. Kitaura and H. Shinohara, Jpn. J. Appl. Phys., Part 1 **46**, 881 (2007).
[4] T. Shimada, Y. Ohno, T. Okazaki, T. Sugai, K. Suenaga, S. Kishimoto, T. Mizutani, T. Inoue, R. Taniguchi, N. Fukui, H. Okubo, and H. Shinohara, Physica E (Amsterdam) **21**, 1089 (2004).
[5] T. Shimada, Y. Ohno, K. Suenaga, T. Okazaki, S. Kishimoto, T. Mizutani, R. Taniguchi, H. Kato, B. P. Cao, T. Sugai, and H. Shinohara, Jpn. J. Appl. Phys., Part 1 **44**, 469 (2005).
[6] G. W. Morley, B. J. Herbert, S. M. Lee, K. Porfyrakis, T. J. S. Dennis, D. Nguyen-Manh, R. Scipioni, J. van Tol, A. P. Horsfield, A. Ardavan, D. G. Pettifor, J. C. Green, and G. A. D. Briggs, Nanotechnology **16**, 2469 (2005).
[7] S. C. Benjamin, A. Ardavan, G. A. D. Briggs, D. A. Britz, D. Gunlycke, J. Jefferson, M. A. G. Jones, D. F. Leigh, B. W. Lovett, A. N. Khlobystov, S. A. Lyon, J. J. L. Morton, K. Porfyrakis, M. R. Sambrook, and A. M. Tyryshkin, J. Phys.: Condens. Matter **18**, S867 (2006).
[8] M. Xiao, L. Martin, E. Yablonovitch, and H. W. Jiang, Nature (London) **430**, 435 (2004).
[9] A. A. R. Watt, M. R. Sambrook, S. V. Burlakov, K. Porfyrakis, and G. A. D. Briggs, e-print arXiv:0810.3124.
[10] H. Shinohara, Rep. Prog. Phys. **63**, 843 (2000).
[11] A. N. Khlobystov, K. Porfyrakis, M. Kanai, D. A. Britz, A. Ardavan, H. Shinohara, T. J. S. Dennis, and G. A. D. Briggs, Angew. Chem., Int. Ed. **43**, 1386 (2004).
[12] T. Brintlinger, Y. F. Chen, T. Durkop, E. Cobas, M. S. Fuhrer, J. D. Barry, and J. Melngailis, Appl. Phys. Lett. **81**, 2454 (2002).
[13] L. C. Venema, J. W. Janssen, M. R. Buitelaar, J. W. G. Wildöer, S. G.

Lemay, and L. P. Kouwenhoven, Phys. Rev. B **62**, 5238 (2000).
[14]J. Kong, A. Cassell, and H. Dai, Chem. Phys. Lett. **292**, 567 (1998).
[15]J. Lee, H. Kim, S. J. Kahng, G. Kim, Y. W. Son, J. Ihm, H. Kato, Z. W. Wang, T. Okazaki, H. Shinohara, and Y. Kuk, Nature (London) **415**, 1005 (2002).
[16]S. Okada, M. Otani, and A. Oshiyama, Phys. Rev. B **67**, 205411 (2003).
[17]Y. Cho, S. Han, G. Kim, H. Lee, and J. Ihm, Phys. Rev. Lett. **90**, 106402 (2003).
[18]L. Ge, B. Montanari, J. H. Jefferson, D. G. Pettifor, N. M. Harrison, and G. A. D. Briggs, Phys. Rev. B **77**, 235416 (2008).
[19]D. H. Cobden, M. Bockrath, P. L. McEuen, A. G. Rinzler, and R. E. Smalley, Phys. Rev. Lett. **81**, 681 (1998).
[20]P. Utko, J. Nygård, M. Monthioux, and L. Noé, Appl. Phys. Lett. **89**, 233118 (2006).
[21]C. H. L. Quay, J. Cumings, S. J. Gamble, A. Yazdani, H. Kataura, and D. Goldhaber-Gordon, Phys. Rev. B **76**, 073404 (2007).
[22]K. Haldrup, M.S. thesis, University of Copenhagen, 2003.
[23]M. H. Rümmeli, M. Löffler, C. Kramberger, F. Simon, F. Fülöp, O. Jost, R. Schönfelder, A. Grüneis, T. Gemming, W. Pompe, B. Büchner, and T. Pichler, J. Phys. Chem. C **111**, 4094 (2007).
[24]J. Nygård, D. H. Cobden, and P. E. Lindelof, Nature (London) **408**, 342 (2000).
[25]M. R. Buitelaar, A. Bachtold, T. Nussbaumer, M. Iqbal, and C. Schönenberger, Phys. Rev. Lett. **88**, 156801 (2002).
[26]C. H. L. Quay, J. Cumings, S. J. Gamble, R. de Picciotto, H. Kataura, and D. Goldhaber-Gordon, Phys. Rev. B **76**, 245311 (2007).
[27]B. Babić and C. Schönenberger, Phys. Rev. B **70**, 195408 (2004).
[28]A. C. Ferrari and J. Robertson, Philos. Trans. R. Soc. London, Ser. A **362**, 2311 (2004).
[29]S. Piscanec, M. Lazzeri, J. Robertson, A. C. Ferrari, and F. Mauri, Phys. Rev. B **75**, 035427 (2007).
[30]S. Piscanec, M. Lazzeri, F. Mauri, A. C. Ferrari, and J. Robertson, Phys. Rev. Lett. **93**, 185503 (2004).
[31]M. Lazzeri, S. Piscanec, F. Mauri, A. C. Ferrari, and J. Robertson, Phys. Rev. B **73**, 155426 (2006).
[32]S. Pisana, M. Lazzeri, C. Casiraghi, K. S. Novoselov, A. K. Geim, A. C. Ferrari, and F. Mauri, Nat. Mater. **6**, 198 (2007).
[33]N. Caudal, A. M. Saitta, M. Lazzeri, and F. Mauri, Phys. Rev. B **75**, 115423 (2007).
[34]Y. Wu, J. Maultzsch, E. Knoesel, B. Chandra, M. Huang, M. Y. Sfeir, L. E. Brus, J. Hone, and T. F. Heinz, Phys. Rev. Lett. **99**, 027402 (2007).
[35]A. C. Ferrari and J. Robertson, Phys. Rev. B **61**, 14095 (2000); **64**, 075414 (2001).
[36]C. Thomsen and S. Reich, Phys. Rev. Lett. **85**, 5214 (2000).
[37]F. Tuinstra and J. L. Koenig, J. Chem. Phys. **53**, 1126 (1970).
[38]R. J. Nemanich and S. A. Solin, Phys. Rev. B **20**, 392 (1979).
[39]A. C. Ferrari, J. C. Meyer, V. Scardaci, C. Casiraghi, M. Lazzeri, F. Mauri, S. Piscanec, D. Jiang, K. S. Novoselov, S. Roth, and A. K. Geim, Phys. Rev. Lett. **97**, 187401 (2006).
[40]A. Jorio, C. Fantini, M. A. Pimenta, R. B. Capaz, Ge. G. Samsonidze, G. Dresselhaus, M. S. Dresselhaus, J. Jiang, N. Kobayashi, A. Grüneis, and R. Saito, Phys. Rev. B **71**, 075401 (2005).
[41]H. Telg, J. Maultzsch, S. Reich, and C. Thomsen, Phys. Rev. B **74**, 115415 (2006).
[42]A. Jorio, R. Saito, J. H. Hafner, C. M. Lieber, M. Hunter, T. McClure, G. Dresselhaus, and M. S. Dresselhaus, Phys. Rev. Lett. **86**, 1118 (2001).
[43]H. Telg, J. Maultzsch, S. Reich, F. Hennrich, and C. Thomsen, Phys. Rev. Lett. **93**, 177401 (2004).
[44]J. Maultzsch, S. Reich, U. Schlecht, and C. Thomsen, Phys. Rev. Lett. **91**, 087402 (2003).